FABRICATION OF HIGH HARDNESS AND HIGH STRENGTH AlTi - TiB_2 COMPOSITE MATERIALS

M. Yoshida

National Institute of Technology, Ube College, 2-14-1 Tokiwadai, Ube, Yamaguchi, Japan
Email: yoshida@ube-k.ac.jp, Web Page: http://www.ube-k.ac.jp/

Keywords: Spark Plasma Sintering, TiB_2, Vickers Hardness, Bending Strength, Crack

Abstract
It has been shown that AlTi-TiB_2 composite in which sub-micron sized TiB_2 particles are dispersed in AlTi matrix can be formed by the reaction sintering of Al-Ti intermetallics and boron powders at 1573K using the spark plasma sintering method. The Vickers hardness of AlTi-76vol%TiB_2 is as high as 2450Hv and the bending strength is 763MPa. By the SEM observation of the Vickers indentation, no crack has been observed indicating good fracture toughness. AlTi-TiB_2 composite specimens have been fabricated using commercialized TiB_2 particles of size of around 2 μm, also. It has been shown that the mechanical properties of AlTi-TiB_2 composite with sub-micron sized TiB_2 particles is superior than those with micron sized TiB_2.

1. Introduction

Titanium diboride (TiB_2) has many desirable properties such as high hardness (Hv=3400), high melting point (3000K), low density, high electrical resistivity and good corrosion resistance[1]. It is a promising candidate for cutting tools, wear proof parts, aircraft propulsion systems, space vehicle thermal protection and so on. However, a high sintering temperature above 2000K is required to obtain TiB_2 of high quality, which limits its application[2-4]. In order to obtain dense and hard TiB_2 based materials by the sintering at lower temperatures, sintering of TiB_2 with various intermetallics as sintering aid has been investigated [5-7]. We have shown that the addition of Al_3Ti improves the mechanical properties of sintered TiB_2[5,6]. The Hv of 2100 and bending strength of 600MPa has been obtained for TiB_2-30vol%Al_3Ti sintered at 1473K [5]. Li et al have shown that dense TiB_2 based material can be obtained by the combustion synthesis using Fe-Al intermetallics as the binder phase. They have shown that TiB_2-20vol%FeAl has hardness of around 1800Hv and bending strength of 630Mpa [7].
It has been reported that the grain size of TiB_2 has a great influence on the mechanical properties of the sintered TiB_2 [2,3]. By the combustion synthesis of Ti and B, grain size becomes larger than 2 μm because of rapid temperature increase associated with the formation of TiB_2. In the present study, it has been shown that AlTi-TiB_2 composite in which sub-micron sized TiB_2 particles are dispersed in AlTi matrix can be formed by the reaction sintering of Al-Ti intermetallic compounds with boron powders using the spark plasma sintering method. We have fabricated AlTi-TiB_2 composite specimens using commercialized TiB_2 particles of size of around 2 μm, also. It has been shown that the mechanical properties of AlTi-TiB_2 composites with sub-micron sized TiB_2 particles are superior than those with micron sized TiB_2.

2. Experimental method

Excerpt from ISBN 978-3-00-053387-7

The raw materials were commercially available Ti powders (99.9% purity and 10μm diameter), Al powders (99.9% and 10μm) and B powders (99% and 10μm). AlTi-TiB_2 composites were fabricated using Al-Ti intermetallics powders and boron powders. Al-Ti intermetallics powders were sinthesized by heating the elemental Al and Ti mixed powders at 923K in a flowing argon atmosphere. It should be noticed that, by this heat treatment, various Al-Ti intermetallic compounds such as AlTi (γ-phase) and $AlTi_3$ (α_2-phase) are formed. We refer to the Al-Ti intermetallic powders by the initial Al:Ti ratio such as $AlTi_2$ or $AlTi_3$, hereafter. A graphite die, having an internal diameter of 20mm and a wall thickness of 10mm was filled with 5g of the mixed powders of (Al+Ti), ($AlTi_2$+B) or ($AlTi_3$+B). Powders were sealed by two graphite punches and mounted on the equipment, LABOX 625 fabricated by Sinterland Ltd. The mixed powders were heated to 1573K with the rate of 50K/min, kept for 20 minutes, and then furnace cooled to room temperature. The temperature was measured using the infrared radiation thermometer IR-AHS0 fabricated by Chino Corporation. Sintering was performed in a vacuum with a residual pressure of 10Pa. A uniaxial pressure of 20MPa was applied during the sintering. We fabricated monolithic AlTi (γ-phase) as well as AlTi-TiB_2 composite using spark plasma sintering method. Sintering of AlTi (γ-phase) was performed using elemental Al and Ti powders. For the sake of comparison, we fabricated AlTi-TiB_2 composites using commerciallized TiB_2 powders of the size of around 2 μm and elemental Al and Ti powders, also. The purity of commerciallized TiB_2 powders was 99.9%.

The microstructure and mechanical properties of the specimens were investigated. Scanning electron microprobe observation was performed using a Hitachi H-4300 instrument. X-ray diffraction patterns were measured using a Rigaku Ultima IV X-ray diffractmeter with Cu-kα radiation source. Vickers hardness was measured using a Shimadzu HMV-2 micro hardness tester with the load of 9.8N and pressing time of 15 seconds. To perform the bending test, rectangular shape samples with the size of 2x3x20 mm^3 were cut by the electric discharge. Three points bending tests were performed using a Shimadzu AGS-J test machine with the crosshead speed of 0.5mm/min and the span of 15mm.

3. Experimental Results and discussion

Figure 1 shows the X-ray diffraction pattern from the (a) (Al+Ti) and (b) (Al+0.6Ti) specimen sintered at 1573K. In the x-ray diffraction pattern of the sintered (Al+Ti) specimen, diffraction peaks from AlTi (γ-phase) and $AlTi_3$ (α_2-phase) has been observed. We have confirmed that the intensity of the diffraction peaks from $AlTi_3$ decreases as the content of Ti in the initial powders decreases. In the diffraction pattern of the sintered (Al+0.6Ti) specimen, peaks from AlTi have been observed but peaks from $AlTi_3$ have not as shown in Fig. 1 (b). Thus, it is conjectured that 40% of Al evaporates during sintering at 1573K for 20min.

Figure 2 shows the X-ray diffraction pattern from the sintered ($AlTi_2$+2B), ($AlTi_2$+2.8B) and ($AlTi_3$+4.8B) specimens. In the x-ray diffraction pattern of the sintered ($AlTi_2$+2B) specimen, diffraction peaks from TiB_2, AlTi (γ-phase) and $AlTi_3$ (α_2-phase) has been observed. On the other hand, in the diffraction pattern of the sintered ($AlTi_2$+2.8B) and ($AlTi_3$+4.8B) specimens, peaks from AlTi and TiB_2 have been observed but peaks from $AlTi_3$ have not. Thus, it has been confirmed that about 40% of Al has evaporated during sintering at 1573K in the case of the sintering of (Al-Ti intermetallics and boron) mixed powders as the sintering of (Al+Ti) powders.

The reaction sintering of ($AlTi_2$+2.8B) and ($AlTi_3$+4.8B) powders can be described as follows,

$$AlTi_2+2.8B=0.4Al(evaporate)+0.6AlTi+1.4TiB_2. \tag{1}$$

$$AlTi_3+4.8B=0.4Al(evaporate)+0.6AlTi+2.4TiB_2. \tag{2}$$

The fraction of TiB_2 in the composite given by eq. (1) is 65vol% (68wt%) and that given by eq.(2) is 76vol% (79wt%). We refer to these specimens as AlTi-65vol%TiB_2 and AlTi-76vol%TiB_2 hereafter.

Excerpt from ISBN 978-3-00-053387-7

Figure 3 shows the SEM images of the polished and etched surfaces of the (a) AlTi-65vol%TiB_2 and (b) AlTi-76vol%TiB_2 specimens sintered at 1573K. In Fig. 3 (a) and (b) it is found that AlTi fills the space between TiB_2 grains and dense specimens are obtained. The size of TiB_2 grains is around 0.4 μm in the AlTi-65vol%TiB_2 specimen and around 0.2 μm in the AlTi-76vol%TiB_2. It seems that the space distribution of TiB_2 grains is more uniform in the AlTi-76vol%TiB_2 than in the AlTi-65vol%TiB_2 Specimens.

Figure 4 (a) shows the SEM image of the Vickers indentation in the AlTi-65vol%TiB_2 specimen. Vickers hardness is estimated as 1850±40Hv from the area of the indentation. Figure 4 (b) shows the magnified image of the enclosed area in Fig. 4 (a). In Fig. 4 (b) a crack is observed to emanate from the indentation corner. The crack runs both in the TiB_2 grains and along the interface between TiB_2 and AlTi matrix.

Fracture toughness, Kc, of brittle materials can be estimated from the length of cracks emanating from corners of the Vickers indentation using the next equation [8],

$$Kc=0.0319P/al^{1/2}\ , \tag{3}$$

where P is the indentation load, a half length of the indentation diagonal and l the crack length. The fracture toughness of AlTi-65vol%TiB_2 is estimated as 12 MPa・$m^{1/2}$ using eq. (3).

Figure 5 (a) shows the SEM image of the Vickers indentation in the AlTi-76vol%TiB_2 specimen. The Vickers hardness of the AlTi-76vol%TiB_2 specimen is estimated as 2450±40Hv. The results of the Vickers tests are summarized in table 1. Figure 5 (b) shows the magnified image of the enclosed area of Fig. 5 (a). In Fig. 5 (b) no crack is observed at the indentation corner indicating good ductility of the specimen.

Figure 6 (a) shows the SEM image of the Vickers indentation in the AlTi-76vol%TiB_2 specimen fabricated using the commercialized TiB_2 particles. The Vickers hardness of this specimen is estimated as 1950Hv which is smaller than that of the AlTi-76vol%TiB_2 with submicron sized TiB_2 particles shown in Fig. 5. Figure 6 (b) shows the magnified image of the enclosed area in Fig. 6 (a). The size of TiB_2 particles in Fig. 6 (b) is around 2μm which is about 10 times larger than that of the specimen fabricated by the reaction synthesis of Al-Ti intermetallics and boron powders (see Figs. 4 and 5). In Fig. 6 (b) it is observed that cracking occurs in the TiB_2 grain located near the indentation corner as shown by an arrow. Since the TiB_2 reinforcing phase is much stiffer than the matrix AlTi phase, a significant fraction of stress is borne by the reinforcement phase. As the size of the reinforcement particle increases, the stress becomes larger, which causes the fracture of the reinforcement particle. The occurrence of cracking causes the degradation of the Vickers hardness.

We have performed three point bending tests of the AlTi-65vol%TiB_2 and AlTi-76vol%TiB_2 specimens with sub-micron and micron sized TiB_2 particles. The results are summarized in table 1. The bending strength of the AlTi-TiB_2 composite of sub-micron sized TiB_2 particles is around 750MPa while that with micron-sized TiB_2 is lower than 500MPa. Cracking of the TiB_2 particles due to the intensified load transfer from the matrix to the reinforcement phases may be responsible for the strength reduction of the AlTi-TiB_2 composite with micron sized TiB_2 particles.

Li et al fabricated FeAl-80vol%TiB_2 composite by the combustion synthesis method and measured the Vickers hardness and fracture toughness [7]. Their value is 1800Hv and 6MPa・$m^{1/2}$. Both of the Vickers hardness and the fracture toughness of AlTi-TiB_2 composite with fine TiB_2 grains is superior than those of FeAl-TiB_2 composite.

Excerpt from ISBN 978-3-00-053387-7

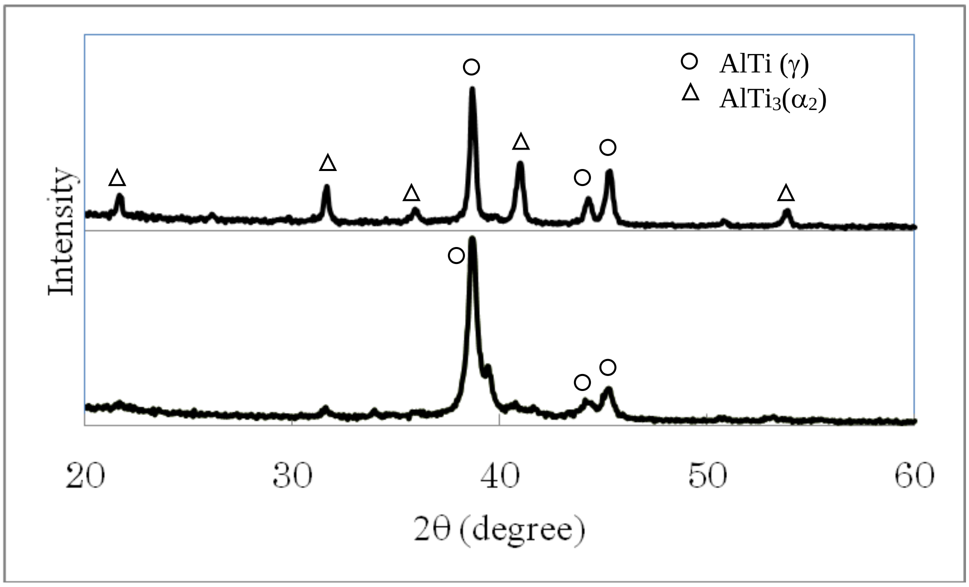

Fig. 1 X-ray diffraction pattern from the sintered (a) (Al+Ti) and (b) (Al+0.6Ti) mixed powder. Open circles indicate diffraction peaks from AlTi (γ-phase) and triangles $AlTi_3$ (α2-phase).

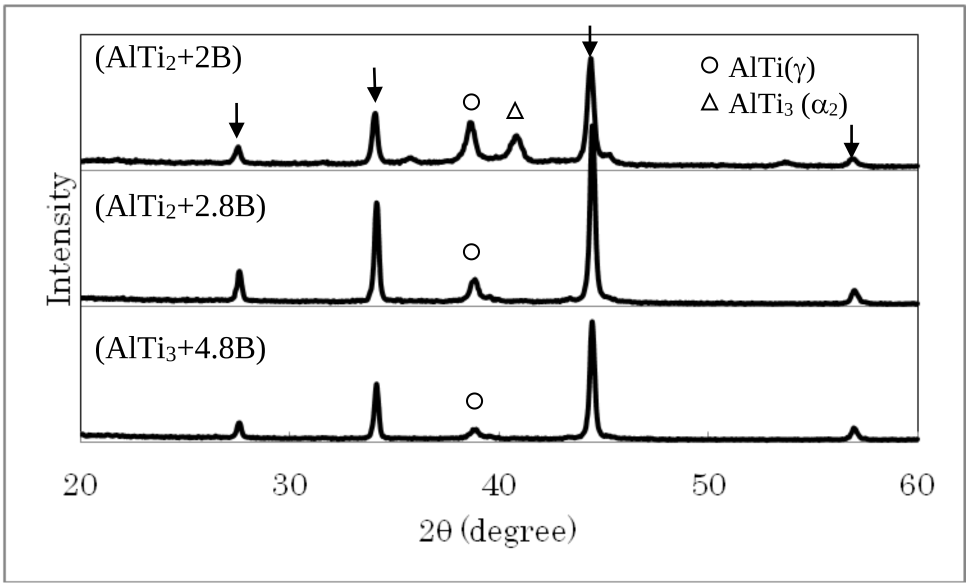

Fig.2 X-ray diffraction pattern from the specimens of sintered ($AlTi_2$+2B) , ($AlTi_2$+2.8B) and ($AlTi_3$+4.8B) mixed powders. Arrows indicate peaks from TiB_2, open circles AlTi (γ-phase) and triangles $AlTi_3$ (α2-phase).

Excerpt from ISBN 978-3-00-053387-7

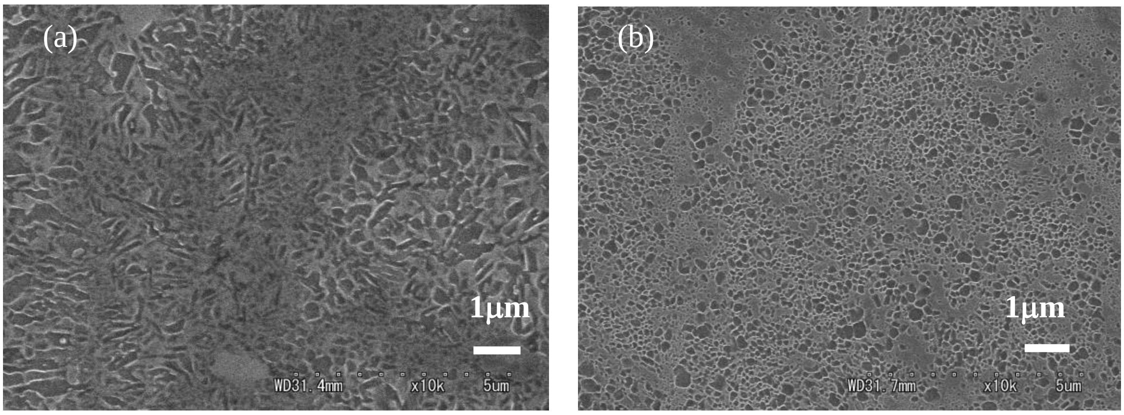

Fig. 3 SEM images of the polished and etched surfaces of the (a) AlTi-65vol%TiB_2 and (b) AlTi-76vol%TiB_2 specimens.

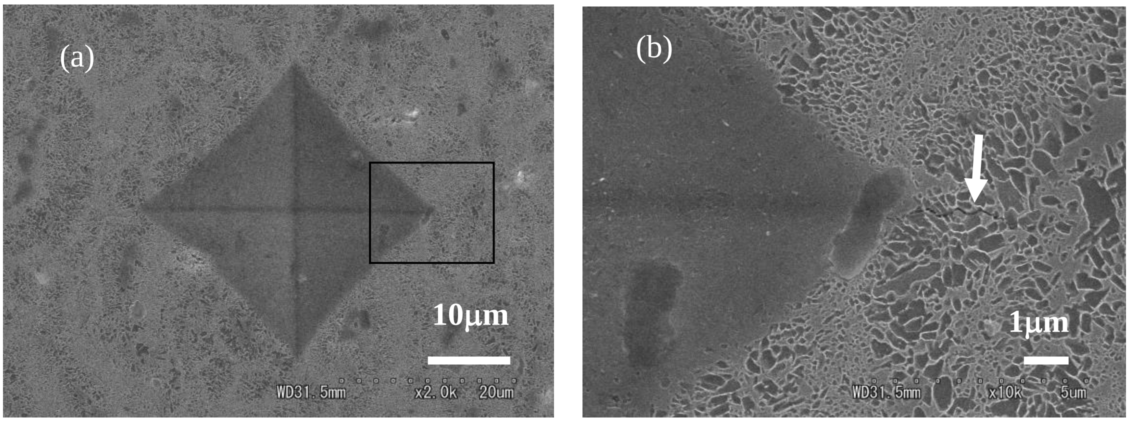

Fig. 4 (a) SEM image of the Vickers indentation in the AlTi-65vol%TiB_2 specimen and (b) the expanded image of the encircled area in (a).

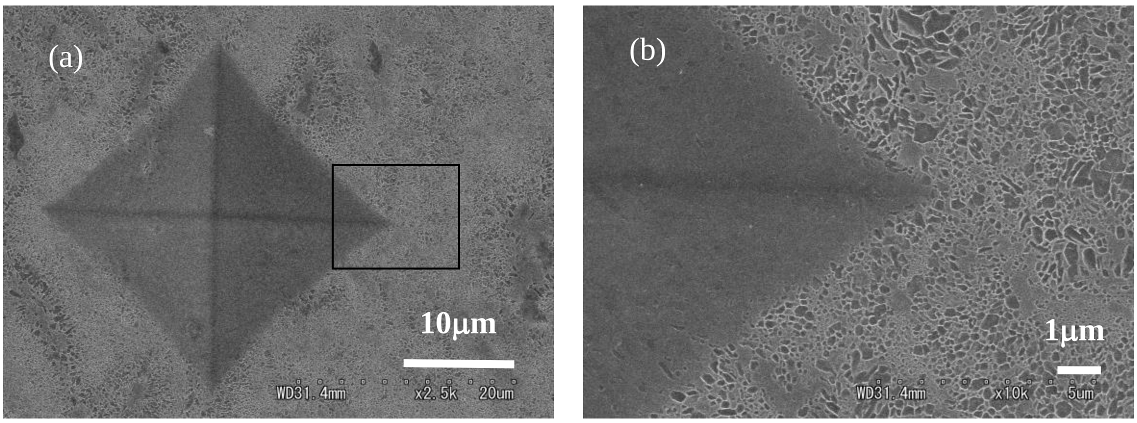

Fig. 5 (a) SEM image of the Vickers indentation in the AlTi-76vol%TiB_2 specimen and (b) the expanded image of the enclosed area in (a).

Excerpt from ISBN 978-3-00-053387-7

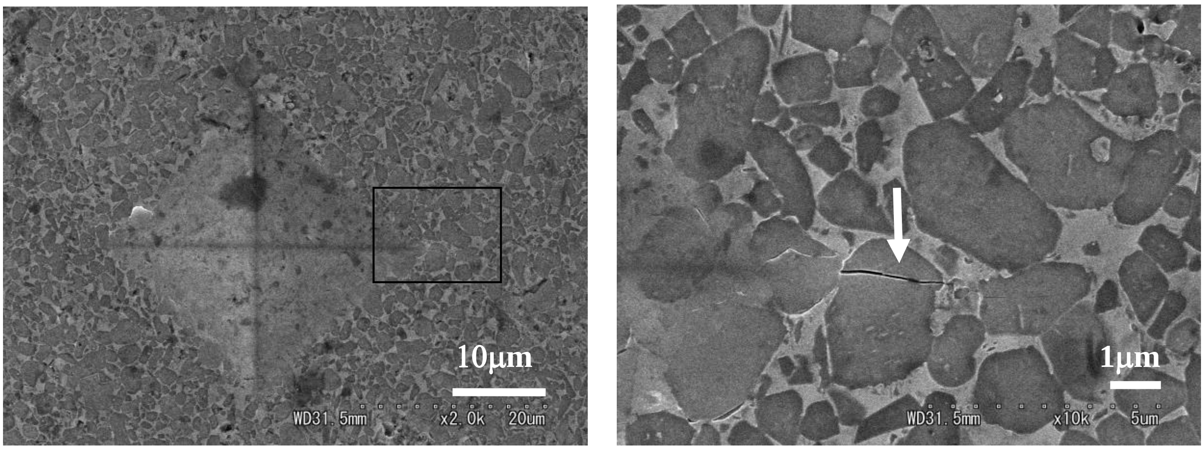

Figure 6 (a) SEM image of the Vickers indentation in the AlTi-76vol%TiB_2 specimen fabricated using commercialized TiB_2 powders and (b) the expanded image of the enclosed area in (a).

Table 1. Mechanical properties of the AlTi-TiB_2 composite specimens sintered at 1573K using spark plasma sintering method.

Starting powders	Composition of the sintered specimen	Vickers Hardness (Hv)	Bending Strength (MPa)	Fracture Toughness (MPa)
$AlTi_2$+2.8B	0.6AlTi+1.4TiB_2 (AlTi-65vol%TiB_2)	1850 ± 40	742 ± 14	12
$AlTi_3$+4.8B	0.6AlTi+2.4TiB_2 (AlTi-76vol%TiB_2)	2450 ± 40	763 ± 20	>20
Al+0.6Ti+2.4TiB_2	0.6AlTi+2.4TiB_2 (AlTi-76vol%TiB_2)	1950 ± 50	496 ± 20	—

4. Conclusions

It has been shown that AlTi-TiB_2 composite in which sub-micron sized TiB_2 particles are dispersed in AlTi matrix can be formed by the reaction sintering of Al-Ti intermetallics and boron powders at 1573K using spark plasma sintering method. It has been confirmed that evaporation of Al occurs during the sintering at 1573K and it is necessary to increase the content of Al in the starting powder to compensate the evaporation of Al. The Vickers hardness of AlTi-76vol%TiB_2 is as high as 2450Hv and the bending strength is 763MPa. By the SEM observation of the Vickers indentation in the AlTi-76vol%TiB_2 specimen, no crack has been observed indicating good ductility. On the other hand, cracking of TiB_2 particles has been observed in the AlTi-76vol%TiB_2 composite fabricated using commercialized TiB_2 particles of size of around 2 μm. It has been shown that the mechanical properties of AlTi-TiB_2 composites with sub-micron sized TiB_2 particles is superior than those with micron sized TiB_2.

Acknowledgments

This work is supported by the Grant-in-Aid for Science Research from Japan Society for the promotion of Science (Kakenhi 25420739)

Excerpt from ISBN 978-3-00-053387-7

References

[1] R.A. Cultuler, Engineering Materials Handbook 4, ASME International, 1991.
[2] W. Wang, Z. Fu, H. Wang and R.J.Yuan, Influence of hot pressing sintering temperature and time on microstructure and mechanical properties of TiB_2 ceramics, European Ceramic Society, 22: 1045-1049, 2002.
[3] A.Mukhopadhyay, G.B.Raju, B.Basu and A.K.Suri, Correlation between phase evolution, mechanical properties and instrumented indentation response of TiB_2-based ceramics, J.Europ. Ceramic Society, 29: 505-516, 2009.
[4] Z.Zhang, X.B.Shen, F.C.Wang, S.K.Lee and L.Wang, Densification behavior and mechanical properties of the spark plasma sintered monolithic TiB_2 ceramics, Material Science and Engineering, A527: 5947-5951, 2010.
[5] M. Yoshida, Influence of sintering temperature on the microstructure of TiB_2 sintered with Al3Ti Additive, Materials Transaction, 53: 1648-1652, 2012.
[6] M. Yoshida and T. Yumitate, Mechanical properties of TiB_2-Al_3Ti and TiB_2-$(Al,Ni)_3Ti$ composites, Material Transaction, 53: 1933-1937, 2012.
[7] Y.Li, K.Matsuura, M.Ohno, Y.M.Gao and J.Yu, Combustion synthesis of TiB_2 based hard material cemented by Fe-Al intermetallics, Powder Metallurgy, 55: 162-167, 2012.
[8] C.B.Ponton and R.D.Rawlings, Vickers indentation fracture toughness test part 1 review of literature and formulation of standardized indentation toughness equations, Material Science and Technologies, 5: 865-872, 1989.

Excerpt from ISBN 978-3-00-053387-7